Journal of Applied Mechanics and Technical Physics, Vol. 39, No. 4, 1998

DETERMINATION OF THE AERODYNAMIC CHARACTERISTICS OF AIRCRAFT IN THE TRANSONIC VELOCITY RANGE

M. A. Naida and A. S. Fonarev

UDC 533.6.011

The problem of determining the integral aerodynamic characteristics of aircraft as a whole in the transonic velocity range is considered. An approximate method of their calculation is developed using the nonlinear transonic theory of small perturbations for three-dimensional flow over a body. The method of investigation consists in separating the flow region into two subregions (outer and inner), applying numerical methods of integrating the equations in those regions, and joining the solutions. The Murman–Cole method of calculating the pressure drag of an isolated wing is generalized to the case of a combination of wing and fuselage.

In the study, within the framework of the theory of small perturbations, of three-dimensional, transonic flows around thin wings with an aspect ratio on the order of unity and of their combination with a fuselage whose maximum cross-sectional size is small compared to its length, it is possible to substantially simplify the statement of the problem of streamline flow by using the technique of joining asymptotic expansions [1]. It was shown in [1] that there are two regions in each of which the flow is described by different boundary-value problems. In the inner region (adjacent to the body), the leading term of the expansion of the potential of the perturbed velocity satisfies a linear Laplace equation in the planes perpendicular to the body's axis. In the outer region, the solution at large distances has an axisymmetric structure and coincides in the leading term with the solution of the problem of flow over an equivalent body of revolution.

The calculation of three-dimensional flow thus comes down to a joint solution of two boundary-value problems for equations in which the unknown function depends on only two spatial variables. Unfortunately, in this case, it is impossible to determine the aircraft's lift, since it is identically zero owing to the axial symmetry of the outer flow. This approach is therefore used mainly to find the pressure distribution over the surface of an aircraft having a small lift [2].

A new statement of the problem, free of the aforementioned drawback, was proposed in [3] to calculate transonic flow over an aircraft having a wing of large aspect ratio. In accordance with [3], in the inner region, in which the flow, as before, is described by the Laplace equation in planes transverse to the body's axis, one places not the entire aircraft but only the fuselage with the tail assembly and part of the wing. The rest of the wing is in the outer region, in which the potential of the perturbed velocity satisfies a three-dimensional analog of the Kàrmàn equation. The integral aerodynamic characteristics of the entire aircraft are determined in such an approach by integrating the pressure distribution over the surface of the body in both regions and then summing the results.

It should be noted that the accuracy of this method of calculating aerodynamic characteristics can be affected by errors due to local violations of the premises of the theory of small perturbations in the vicinity of the leading blunt edges of the wing and the tail assembly, near the fuselage nose, etc. As calculations show [4], in determining the lift coefficients and the pitching moment, the influence of these local errors is slight and the results have acceptable accuracy. A different situation arises in determining the body's drag by numerical integration of the pressure distribution over its surface. It is well known [5] that the result of numerical

Central Aerohydrodynamics Institute, Zhukovskii 140160. Translated from Prikladnaya Mekhanika i Tekhnicheskaya Fizika, Vol. 39, No. 4, pp. 91–101, July–August, 1998. Original article submitted October 9, 1996.

0021-8944/98/3904-0559 $20.00

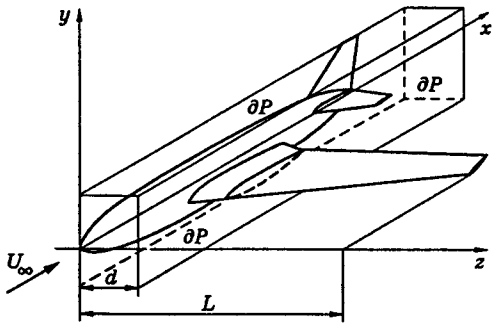

Fig. 1

integration in this case may prove inaccurate and even negative, since in the integration one has to calculate the difference between two large quantities but with close values. To increase the accuracy in determining the drag coefficient of wing profiles and thin wings in [5], the procedure of integrating the pressure distribution over the body's surface was changed to another procedure that does not use integration at points of possible violation of the premises of the theory of small perturbations. A similar approach was used in [6] to calculate the wave drag of bodies of revolution. In [7, 8], the method of [5] was generalized to the case of nonsteady transonic flow over thin wing profiles and bodies of revolution.

In the present work, we consider the problem of determining the integral aerodynamic characteristics of an aircraft as a whole in the transonic velocity range. An approximate method of their calculation is developed, based on the use of the nonlinear transonic theory of small perturbations for three-dimensional flow over bodies. The method of investigation consists in separating the flow region into two subregions (outer and inner), applying numerical methods of integration of the equations in those regions, and joining the solutions. The Murman–Cole method of calculating the pressure drag of an isolated wing is generalized to the case of a wing–fuselage combination.

The following aerodynamic characteristics were calculated: drag, lift, and pitching moment for a specific aircraft makeup of fuselage, swept wing, and tail assembly. A comparison is made with experimental data.

1. Formulation of the Problem. Let an inviscid, transonic gas stream with a velocity U_∞ at infinity flow over the aircraft. We place the origin of the right-handed Cartesian coordinate system at the nose of the fuselage and direct the x axis from the nose toward the tail section, the y axis upward, and the z axis along the wingspan (Fig. 1). We also consider three-dimensional transonic flows in which the compression shocks that develop are weak, so that the changes in entropy in gas particles crossing their fronts can be neglected. In this case, the gas flow is described by the velocity potential

$$\Phi = U_\infty l(x\cos\alpha + y\sin\alpha + \varphi),$$

where l is the length of the fuselage, α is the angle of attack, and φ is the potential of the perturbations. Within the framework of the theory of small perturbations, the dimensionless potential φ satisfies the three-dimensional analog of the Kàrmàn equation,

$$((C_1 + C_2\varphi_x)\varphi_x)_x + \varphi_{yy} + \varphi_{zz} = 0. \tag{1.1}$$

Here $C_1 = 1 - \mathrm{M}_\infty^2$ and $C_2 = -(\gamma+1)\mathrm{M}_\infty^2/2$; all the independent variables are normalized to l.

Let the angle of yaw be zero. Since the aircraft is symmetrical about the xy plane, we consider the flow only in the half-space $z \geqslant 0$. Along the x axis we isolate a parallelepiped P, inside which we place the fuselage and tail assembly and part of the wing (Fig. 1). In accordance with the asymptotic theory of [1], the potential of perturbations within P satisfies the Laplace equation in any plane $x = \text{const}$. To emphasize the two-dimensional character of the solution, we introduce a new designation of the perturbation potential $\psi(x, y, z)$ for this region. In this case, we have

$$\psi_{yy} + \psi_{zz} = 0. \tag{1.2}$$

Outside of P the flow is three-dimensional and is described by a potential φ that satisfies Eq. (1.1). To join the inner and outer solutions at the surface ∂P of the parallelepiped, we set up the condition of continuity of the potential and its derivative along the normal to the faces of P:

$$\varphi = \psi, \quad x, y, z \in \partial P; \tag{1.3}$$

$$\varphi_n = \psi_n, \quad x, y, z \in \partial P. \tag{1.4}$$

At the body's surface, the perturbation potential must satisfy the condition of nonpenetration. For the part of the aircraft inside P, the nonpenetration condition $\mathbf{V} \cdot \mathbf{N} = 0$ ($\mathbf{N}$ is the vector of the unit outward normal to the body's surface) takes the form

$$(\cos\alpha + \psi_x)N_x + (\sin\alpha + \psi_y)N_y + \psi_z N_z = 0, \tag{1.5}$$

where N_x, N_y, and N_z are the projections of $\mathbf{N}$ onto the respective axes of the Cartesian coordinate system. Let the angle of attack be small. Then, in accordance with the theory of small perturbations, Eq. (1.5) reduces to

$$N_x + \alpha N_y = -\psi_y N_y - \psi_z N_z. \tag{1.6}$$

Since we have $(\psi_y N_y + \psi_z N_z)/\sqrt{N_y^2 + N_z^2} = \psi_n$ ($\mathbf{n}$ is the projection of $\mathbf{N}$ onto the plane $x = \text{const}$), the condition of nonpenetration at the body inside P has the form

$$\psi_n = -(N_x + \alpha N_y)/\sqrt{N_y^2 + N_z^2}. \tag{1.7}$$

Condition (1.7) is specified directly at the body's surface.

Let us now consider the part of the wing that projects beyond P. Since $N_z \ll N_x$ and $N_z \ll N_y$ for the wing, relation (1.5) reduces to the equation $N_x + (\alpha + \varphi_y)N_y = 0$. Let the wing surface be described by the equation $y = y(x, z)$. We then have $N_x/N_y = -y_x$. The condition of nonpenetration at the wing is thus

$$\varphi_y = y_x - \alpha. \tag{1.8}$$

In contrast to (1.7), condition (1.8) is not set at the upper and lower wing surfaces but pertains to the plane $y = y_w$ midway between them. A vortex sheet lies downstream from the trailing edge of the wing. In the theory of small perturbations, it does not depart from the plane $y = y_w$ and extends to infinity. The discontinuity in the potential in the transition through the sheet is determined by the equation

$$\varphi(x, y_w + 0, z) - \varphi(x, y_w - 0, z) = [\varphi] = \Gamma(z), \tag{1.9}$$

where Γ is the velocity circulation near the corresponding wing cross section.

In the Trefftz plane, as $x \to \infty$, the perturbation potential satisfies the Laplace equation and condition (1.9) on the segment $y = y_w$, $d \leqslant z \leqslant L$ [L is the half-wingspan and d is the width of P (Fig. 1)]. The following conditions are satisfied in the plane of symmetry $z = 0$:

$$\psi_z = 0; \tag{1.10}$$

$$\varphi_z = 0. \tag{1.11}$$

Since the outer problem is solved numerically by the time-like iteration method using an equation containing nonsteady terms, to specify the conditions at the outer boundaries of the calculation region (except for the Trefftz plane) we can use the method described in [8]. As a result, we obtain

$$C\varphi_x - \mathrm{M}_\infty(\mathrm{M}_\infty + \sqrt{C + \mathrm{M}_\infty^2})\varphi_t = 0 \quad \text{as} x \to -\infty; \tag{1.12}$$

$$\mathrm{M}_\infty\varphi_y - \sqrt{C}\sqrt{C + \mathrm{M}_\infty^2}\varphi_x = 0 \quad \text{as} \quad y \to -\infty; \tag{1.13}$$

$$\mathrm{M}_\infty\varphi_y + \sqrt{C}\sqrt{C + \mathrm{M}_\infty^2}\varphi_x = 0 \quad \text{as} \quad y \to \infty; \tag{1.14}$$

$$\mathrm{M}_\infty\varphi_z + \sqrt{C}\sqrt{C + \mathrm{M}_\infty^2}\varphi_x = 0 \quad \text{as} \quad z \to \infty, \tag{1.15}$$

where $C = C_1 + 2C_2\varphi_x$.

We thus formulate a mixed boundary-value problem with boundary conditions (1.3), (1.7), and (1.10) in the inner region for Eq. (1.2). In formulating the boundary-value problem in the outer region, we use relations (1.4), (1.8), and (1.11)–(1.15) as the boundary conditions for Eq. (1.1). The distribution of the potential φ satisfying the Laplace equation and condition (1.9) is specified in the Trefftz plane.

After the perturbation potential has been determined, the pressure coefficient in the inner region has the form [9]

$$c_p = -2\psi_x - \psi_y^2 - \psi_z^2 \tag{1.16}$$

and the pressure coefficient in the outer region has the form

$$c_p = -2\varphi_x. \tag{1.17}$$

2. Determination of Aerodynamic Characteristics. Suppose that the boundary-value problems formulated in the outer and inner regions have been solved. Let us determine the integral aerodynamic characteristics of the aircraft: the lift c_y, the pressure drag c_x, and the pitching moment m_z. In the associated coordinate system adopted, these characteristics are found as follows:

$$c_y = \frac{2F_y}{\rho_\infty U_\infty^2 l^2} = -2\iint\limits_s c_p(\mathbf{N}\cdot\mathbf{j})\,ds; \tag{2.1}$$

$$c_x = \frac{2F_x}{\rho_\infty U_\infty^2 l^2} = -2\iint\limits_s c_p(\mathbf{N}\cdot\mathbf{i})\,ds; \tag{2.2}$$

$$m_z = \frac{2\mathrm{M}_z}{\rho_\infty U_\infty^2 l^3} = -2\iint\limits_s c_p((\mathbf{N}\cdot\mathbf{j})(x-x_*) - (\mathbf{N}\cdot\mathbf{i})(y-y_*))\,ds. \tag{2.3}$$

Here x_* and y_* are the coordinates of the point in the plane $z = 0$ about which the moment is calculated. Let us first consider the inner region. In this case, s is the surface area of the part of the aircraft inside P, and the coefficient c_p is related to the perturbation potential by (1.16). To determine the vector N, we introduce a parametric representation of the aircraft's surface that follows from a property of the statement of the inner boundary-value problem. We change to a cylindrical coordinate system and as the first parameter we take the angle β reckoned clockwise from the y axis, looking from the nose of the fuselage. The second parameter ξ coincides identically with x. The Cartesian coordinates of any point of the surface are then expressed in terms of the respective parameters as follows:

$$x = \xi, \qquad y = y(\beta,\xi), \qquad z = z(\beta,\xi).$$

Let $\mathbf{r} = x\mathbf{i} + y\mathbf{j} + z\mathbf{k}$ be the radius vector of some point on the surface. If this point is not singular, there are two vectors, not parallel to each other, $\mathbf{r}_\beta$ and $\mathbf{r}_\xi$, that lie in the plane tangent to the surface at the given point. In this case, their normalized vector product yields the vector N:

$$\mathbf{N} = \frac{\mathbf{r}_\beta \times \mathbf{r}_\xi}{|\mathbf{r}_\beta \times \mathbf{r}_\xi|} = \frac{(y_\beta z_\xi - y_\xi z_\beta)\mathbf{i} + z_\beta\mathbf{j} + y_\beta\mathbf{k}}{\sqrt{(y_\beta z_\xi - y_\xi z_\beta)^2 + z_\beta^2 + y_\beta^2}}.$$

Since an element of surface area is defined by the equation $ds = |\mathbf{r}_\beta \times \mathbf{r}_\xi|\,d\beta\,d\xi$, the expressions for the integral aerodynamic characteristics in the inner region take the form

$$c_y = -2\int_0^1\int_0^\pi c_p z_\beta\,d\beta\,d\xi; \tag{2.4}$$

$$c_x = -2\int_0^1\int_0^\pi c_p(y_\beta z_\xi - y_\xi z_\beta)\,d\beta\,d\xi; \tag{2.5}$$

$$m_z = -2\int_0^1\int_0^\pi c_p(z_\beta(x-x_*) - (y_\beta z_\xi - y_\xi z_\beta)(y-y_*))\,d\beta\,d\xi. \tag{2.6}$$

Let us now consider the outer region. To determine c_y, c_x, and m_z from Eqs. (2.1)–(2.3) in this case, we must understand s to be the surface area of that part of the wing that projects beyond P, and c_p is calculated from (1.17). If the wing surface is given by the equation $y = y(x,z)$, the unit normal vector is $\mathbf{N} = (-y_x\mathbf{i} + \mathbf{j} - y_z\mathbf{k})/\sqrt{1+y_x^2+y_z^2}$.

We shall determine the moment relative to a point lying in the wing plane, i.e., $y_* = y_w$. In this case, substituting the expression for N into (2.1)–(2.3) and taking into account that $y_x^2 + y_z^2 \ll 1$ for thin wings, we have the equations

$$c_y = -2\int_d^L\int_{x_l}^{x_t}(c_p^+ - c_p^-)\,dx\,dz; \tag{2.7}$$

$$c_x = -2\int_d^L\int_{x_l}^{x_t}(y_x^+c_p^+ - y_x^-c_p^-)\,dx\,dz; \tag{2.8}$$

$$m_z = -2\int_d^L\int_{x_l}^{x_t}(c_p^+ - c_p^-)(x-x_*)\,dx\,dz, \tag{2.9}$$

where $x_l(z)$ and $x_t(z)$ are the coordinates of the leading and trailing edges of the wing; the superscripts plus and minus pertain to the upper and lower wing surfaces.

Integrals (2.4)–(2.9) are calculated numerically. Since the integrands in (2.5) and (2.8) are sign-variable, in such an approach the drag in each region is obtained as a small difference between two large quantities, and the result of the numerical integration, as noted above, can prove to be inaccurate. To increase the accuracy in determining the drag coefficient, one should, using the integral theorem of momenta, change from the pressure integral over the body to an expression containing integrals over other surfaces having sign-constant integrands. A fairly detailed derivation of such an expression is given in [4] for the case of an isolated wing where the region is single and the entire flow is described by the Kàrmàn equation. Let us see how the result of [4] can be generalized to the case of a combination of wing and fuselage with allowance for the features of the statement of the boundary-value problems in both regions.

The components of the velocity perturbations in the outer region satisfy the system of equations

$$(C_1u + C_2u^2)_x + v_y + w_z = 0, \quad u_y - v_x = 0, \quad u_z - w_x = 0. \tag{2.10}$$

Multiplying the first equation of this system by u, the second by v, and the third by w and adding them, we obtain following relation in divergent form:

$$(C_1u^2/2 + 2C_2u^3/3 - (v^2+w^2)/2)_x + (uv)_y + (uw)_z = 0.$$

Integrating this relation over the entire outer region except for compression shocks and using the Ostrogradskii–Gauss theorem, with allowance for the asymptotic behavior of the far field [4] we have

$$-\iint_{tf\setminus g}\frac{v^2+w^2}{2}\,dy\,dz + \iint_{sh}\left\{\left[C_1\frac{u^2}{2} + \frac{2}{3}C_2u^3 - \frac{v^2+w^2}{2}\right](\mathbf{N}\cdot\mathbf{i}) + [uv](\mathbf{N}\cdot\mathbf{j}) + [uw](\mathbf{N}\cdot\mathbf{k})\right\}ds$$

$$+ \iint_w\{(uv)^- - (uv)^+\}\,dx\,dz + \iint_{\partial P}u\frac{\partial\varphi}{\partial N}\,ds = 0. \tag{2.11}$$

Here the indices tf, g, sh, w, and ∂P denote the Trefftz plane, the trailing end of P, the shock wave, the wing, and the lateral faces of P, respectively; N is the outward normal to the respective surface in the outer region; the square brackets in the integral over the shock wave denote the difference between quantities before and after the shock. With allowance for boundary condition (1.8) and Eqs. (1.17) and (2.8), the integral over the

wing represents the pressure drag in the velocity coordinate system for the part of the aircraft in the outer region:

$$\iint\limits_{w} \{(uv)^- - (uv)^+\}\, dx\, dz = \frac{c_{xa}^w}{4}.$$

Let us consider the integral over the shock. To simplify it, we use the equations for the shock that follow from the divergent form of system (2.10):

$$[C_1 u + C_2 u^2](\mathbf{N}\cdot\mathbf{i}) + [v](\mathbf{N}\cdot\mathbf{j}) + [w](\mathbf{N}\cdot\mathbf{k}) = 0,\ -[v](\mathbf{N}\cdot\mathbf{i}) + [u](\mathbf{N}\cdot\mathbf{j}) = 0,\ -[w](\mathbf{N}\cdot\mathbf{i}) + [u](\mathbf{N}\cdot\mathbf{k}) = 0.$$

Multiplying the first of these conditions by the arithmetic mean $\langle u\rangle$ over the shock, the second by $\langle v\rangle$, and the third by $\langle w\rangle$ and substituting them into the integral over the shock, we can reduce Eq. (2.11) to the form

$$-\iint\limits_{tf\setminus g} \frac{v^2+w^2}{2}\, dy\, dz - \frac{\gamma+1}{12}\mathrm{M}_\infty^2 \iint\limits_{sh} [u]^3\, dy\, dz + \frac{c_{xa}^w}{4} + \iint\limits_{\partial P} u\frac{\partial\varphi}{\partial N}\, ds = 0. \tag{2.12}$$

Equation (2.12) differs from the equation for the pressure drag of an isolated wing in the velocity coordinate system [4] by the presence of an integral over the lateral faces of the parallelepiped P, which is due to the division of the flow into two regions. To eliminate this integral, let us consider the inner region.

The components of the perturbed velocity in the inner region satisfy the system of equations

$$v_y + w_z = 0, \quad u_y - v_x = 0, \quad u_z - w_x = 0. \tag{2.13}$$

Multiplying the first equation of this system by u, the second by v, and the third by w and adding them, we obtain the following equation in divergent form:

$$-((v^2+w^2)/2)_x + (uv)_y + (uw)_z = 0.$$

Integrating this equation over the entire inner region except for the compression shocks and using the Ostrogradskii–Gauss theorem, with allowance for the conditions at the near and far ends of P, we have

$$-\iint\limits_{g} \frac{v^2+w^2}{2}\, dy\, dz + \iint\limits_{sh} \left\{ -\left[\frac{v^2+w^2}{2}\right](\mathbf{N}\cdot\mathbf{i}) + [uv](\mathbf{N}\cdot\mathbf{j}) + [uw](\mathbf{N}\cdot\mathbf{k})\right\} ds$$

$$+ \iint\limits_{f} \left\{ -\frac{v^2+w^2}{2}(\mathbf{N}\cdot\mathbf{i}) + uv(\mathbf{N}\cdot\mathbf{j}) + uw(\mathbf{N}\cdot\mathbf{k})\right\} ds + \iint\limits_{\partial P} u\frac{\partial\psi}{\partial N}\, ds = 0, \tag{2.14}$$

where f denotes integration over the surface of the part of the aircraft inside P and N is the unit normal to the corresponding surface in the inner region. Let us consider the integral over the surface of the body in more detail. In accordance with condition (1.6), it can be represented in the form

$$\iint\limits_{f} \left\{ -\frac{v^2+w^2}{2}(\mathbf{N}\cdot\mathbf{i}) - u(\mathbf{N}\cdot\mathbf{i}) - u\alpha(\mathbf{N}\cdot\mathbf{j})\right\} ds.$$

Since we assume the angle of attack to be small, the drag coefficient in the velocity coordinate system is expressed in terms of the drag and lift coefficients in the associated coordinate system as follows:

$$c_{xa} = c_x + \alpha c_y.$$

Therefore, taking (1.16), (2.1), and (2.2) into account, we can conclude that the integral over the body in the inner region represents with accuracy to higher-order terms the pressure drag in the velocity coordinate system for the part of the aircraft inside P:

$$-\iint\limits_{f} \left\{ \left(\frac{v^2+w^2}{2} + u\right)(\mathbf{N}\cdot\mathbf{i}) + u\alpha(\mathbf{N}\cdot\mathbf{j})\right\} ds = \frac{c_{xa}^f}{4}.$$

Let us now turn to the integral over the shock. To simplify it, we use the equations for the shock that follow from the divergent form of system (2.13):

$$[v](\mathbf{N}\cdot\mathbf{j})+[w](\mathbf{N}\cdot\mathbf{k})=0,\quad -[v](\mathbf{N}\cdot\mathbf{i})+[u](\mathbf{N}\cdot\mathbf{j})=0,\quad -[w](\mathbf{N}\cdot\mathbf{i})+[u](\mathbf{N}\cdot\mathbf{k})=0.$$

Multiplying the first condition by $\langle u\rangle$, the second by $\langle v\rangle$, and the third by $\langle w\rangle$ and substituting them into the integrand, we find that the integral over the shock in the inner region is identically equal to zero. Adding (2.12) and (2.14), we find the expression connecting the drag of the entire aircraft in the velocity coordinate system with the integral over the shock in the outer region and with the integral over the Trefftz plane:

$$c_{xa}=\frac{\gamma+1}{3}\,\mathrm{M}_\infty^2\iint\limits_{sh}[u]^3\,dy\,dz+2\iint\limits_{tf}(v^2+w^2)\,dy\,dz. \tag{2.15}$$

Note that the integrals over the lateral faces ∂P of the parallelepiped for the outer and inner regions cancel out when combined because of conditions (1.3) and (1.4) and the opposite directions of the outward normals.

The first term in (2.15) differs from zero only if the flow over the aircraft is accompanied by the formation of shock waves. It therefore represents the wave drag. The second term in (2.15) represents the induced drag, which differs from zero even in the absence of shocks. This expression for the induced drag coincides with the corresponding result of the linear theory.

3. Numerical Methods of Solving the Problem. We use the panel method [2] to solve the boundary-value problem in the inner region. In this method, the combination of profiles of the body's cross section and the cross section of the parallelepiped P with the plane $x=x_i$ is replaced by a set of flat panels, representing simple layers of sources with a constant intensity. The vortex sheet propagating downstream from the trailing edge of the part of the wing inside P is modeled by a set of doublet panels lying in the plane $y=y_w$ and representing double layers of constant intensity, which is found, in accordance with (1.9), as a jump in the potential at the trailing edge of the wing. To determine the intensities of the simple layers, we use boundary conditions (1.3), (1.7), and (1.10). The boundary conditions are satisfied at the center of each panel to obtain a closed system of equations with a compact matrix for any cross section $x_i=\text{const}$. Since the vectors on the right sides in this case depend, in accordance with (1.3), on the distribution of the potential φ in the outer region, which in turn is found by the time-like iteration method, the system of linear equations in the inner region must be solved repeatedly. The most laborious part of solving the system of linear equations by the Gauss exclusion method is reducing the matrix to triangular form. To avoid the multiple repetition of this procedure and increase the accuracy of the solution, one should use the alternative method of LU expansion with the choice of a leading element over the entire matrix. In this case, it is sufficient to make a LU expansion of each matrix only once.

Let us consider the finite-difference method used to solve the boundary-value problem in the outer region. Since the problem is solved by the time-like iteration method, we start from the following equation containing nonsteady terms:

$$\mathrm{M}_\infty^2\varphi_{tt}+2\mathrm{M}_\infty^2\varphi_{xt}=((C_1+C_2\varphi_x)\varphi_x)_x+\varphi_{yy}+\varphi_{zz}. \tag{3.1}$$

To approximate the nonlinear part of Eq. (3.1), we use a monotonic Engquist–Osher scheme of first-order accuracy [10], and the linear differential operators are approximated by central-difference expressions. The resulting system of grid equations is solved using the method of approximate factoring of a three-dimensional, finite-difference operator. In this method, the three-dimensional, finite-difference operator is represented approximately as the product of three one-dimensional operators [11].

Thus, in performing one step of time integration, one must solve one system of linear equations with a four-diagonal matrix (the x pass) and two systems of linear equations with three-diagonal matrices (the y and z passes). To solve systems of linear equations with diluted matrices of such structure in which all the diagonals are adjacent to the main diagonal, the scalar trial-run method is used. Stability of a scalar trial run requires that the matrix have the property of diagonal dominance. In making the y and z passes, this property is satisfied unconditionally. The higher-order term, from the standpoint of the theory of small perturbations, $\mathrm{M}_\infty^2\varphi_{tt}$ is retained in Eq. (3.1) to ensure diagonal dominance in the x pass.

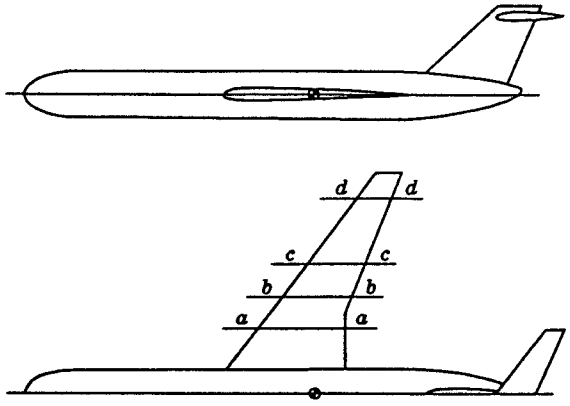

Fig. 2

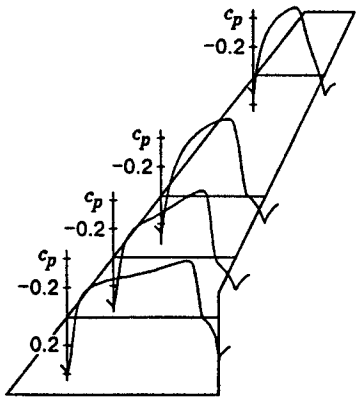

Fig. 3

4. Results of Calculation of Aircraft's Aerodynamic Characteristics. Let us consider the flow over a model of a passenger aircraft shown in Fig. 2 in the range $0.82 \leqslant M_\infty \leqslant 0.98$ with $\alpha = 0$ and 4°. The model is built on the center-section scheme, the wing-sweep angle along the leading edge is $\chi = 37°$, the wing taper is $\eta = 3.64$, the elongation is $\lambda = 7.58$, and the wing has a symmetric P-114s profile. The tail assembly also has a symmetric NACA0010M profile. The stabilizer is set at a $-3°$ angle to the longitudinal axis of the fuselage whose cross sections are circles.

Figure 3 gives the distribution of the pressure coefficient c_p over the wing surface in four cross sections (a–d) shown in Fig. 2 for $\alpha = 0$ and $M_\infty = 0.95$. An analysis of Fig. 3 shows that the point of minimum pressure in cross sections a–d stands a distance from the trailing edge of the wing of 34.1, 38.3, 49.5, and 52% of the length of the local chord of the profile, respectively. Consequently, in base cross sections of the wing, the region of reduced pressure shifts toward the trailing edge of the wing, while in end cross sections it shifts toward the leading edge.

As a result of this, in base cross sections of the wing, the pressure forces on the leading part of the profile increase while those on the trailing part decrease. The pressure drag coefficient therefore takes large positive values in these cross sections. In end cross sections, the shift of the region of maximum rarefaction toward the nose of the profile decreases the pressure forces acting on the nose part of the profile and increases those acting on the tail part. The pressure drag coefficient thus decreases considerably in the end cross sections, becoming negative. In intermediate cross sections of the wing, the local drag coefficient changes from positive to negative. This relationship has also been observed experimentally [12, p. 57].

Let us examine how this behavior of the c_p distribution over the wing surface affects the accuracy in determining the pressure drag coefficient. We determine c_x by numerical integration in accordance with (2.8). We first integrate over the x variable, i.e., in wing cross sections $z = \text{const}$. In this case, the integrand is sign-variable and the drag coefficient for the cross section is obtained as a small difference between two large quantities: the drag on the nose part of the profile and the thrust exerted on its tail part. Since the distribution of the drag coefficients of individual cross sections along the wingspan, as shown above, is also a sign-variable function, in the integration over the z variable, the drag coefficient of the wing as a whole is again obtained as a small difference of two large quantities. As a result, a buildup of numerical errors occurs that can result in the drag coefficient being obtained with a large error.

Figure 4 shows calculated and experimental curves of c_x, c_y, and m_z as functions of M_∞ for $\alpha = 0$. Curve 1 corresponds to the value of c_x calculated by the method of integration over the shock in accordance with (2.15), curve 2 is experimental, calculated as the difference between the total drags for the given Mach number and $M_\infty = 0.6$ for the subcritical flow regime, and curve 3 was determined by the method of integration over the body, i.e., as the sum of (2.5) and (2.8). The calculated lift is given by curve 4. In the case under consideration, the lift is produced mainly by the horizontal tail and has a small negative value because of the

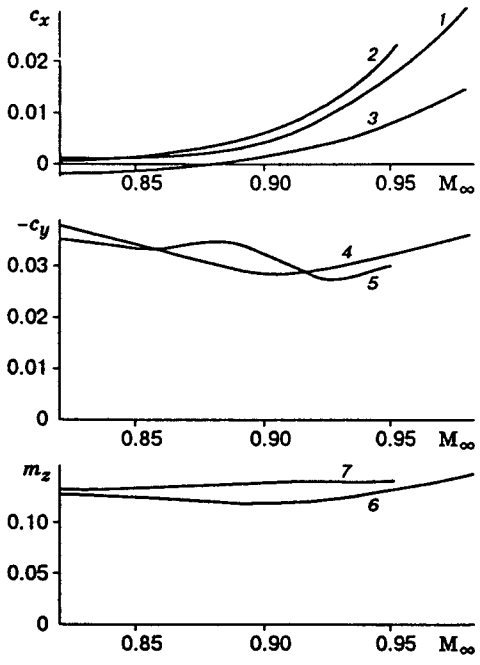

Fig. 4

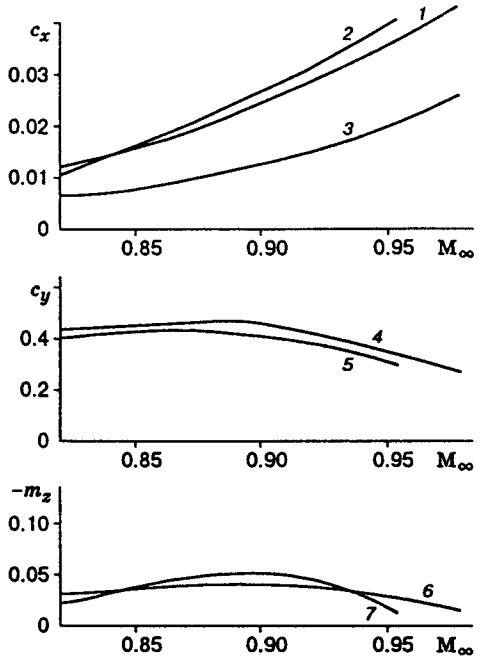

Fig. 5

negative mounting angle of the stabilizer. A comparison of the calculated curve 4 and the experimental curve 5 shows that they are fairly close to each other, except for the range $0.87 \leqslant M_\infty \leqslant 0.92$. This discrepancy is probably related to the influence of viscosity effects.

Curves 6 and 7 in Fig. 4 represent the calculated and experimental behavior of the pitching moment. In both cases, the pitching moment is determined relative to the center of gravity of the model, whose position is shown in Fig. 2. Because the shape of the fuselage is nearly axisymmetric, the model was built on the center-section scheme and $y_* = y_w$, the pitching moment is produced mainly by aerodynamic forces exerted on the tail assembly. A comparison of the calculated and experimental functions $m_z(M_\infty)$ suggests that the drag forces produced by gas viscosity and not taken into account in this statement of the problem, make a considerable contribution to the total moment. We note that the calculated curve understates the value of m_z, since viscous friction exerted on the tail assembly produces a moment of the same sign as the lift.

Figure 5 gives calculated and experimental dependences of the aircraft's aerodynamic characteristics on M_∞ for $\alpha = 4°$ in the velocity coordinate system. The curves have the same designations as in Fig. 4. Since the wing produces a great lift in this case (curves 4 and 5), in determining the experimental values of the pressure drag, we must allow for the contribution of induced drag. Therefore, in contrast to the case of $\alpha = 0$, curve 2 was calculated as the total drag at the given Mach number minus the difference between the total and induced drags at $M_\infty = 0.6$. The induced drag was calculated from Eq. (2.15) by numerical solution of the auxiliary problem of streamline flow.

On the whole, the comparison of experimental and calculated aerodynamic characteristics of the aircraft under consideration enables us to conclude that they are in satisfactory agreement. Note that the pressure drag is determined with acceptable accuracy only by the method of integration over the shock.

This work was supported by the Russian Foundation for Fundamental Research (Grant No. 95-01-01067a).

REFERENCES

1. K. Oswatitsch and F. Keune, "Ein Aquivalenzsatz fur nichtangestelle Flugel kleiner Spannweite in Schallnaher Stromung," *Z. Flugwiss.*, **3**, No. 2, 23–48 (1955).
2. N. D. Malmuth, C. C. Wu, and J. D. Cole, "Slender body theory and space shuttle transonic aerodynamics," AIAA Paper No. 85-0478 (1985).
3. U. G. Navert and Y. C. Sedin, "Transonic computations about complex configurations using coupled inner and outer flow equations," in: *Proc. of the 15th ICAS Congress*, Vol. 1 (1986), pp. 303–312.
4. J. D. Cole and L. P. Cook, Transonic Aerodynamics, Elsevier, Dordrecht (1986).
5. E. M. Murman and J. D. Cole, "Inviscid drag at transonic speeds," AIAA Paper No. 74-0540 (1974).
6. M. A. Naida and A. S. Fonarev, "An effective method of calculating the wave drag of bodies of revolution in the transonic range," *Prikl. Mekh. Tekh. Fiz.*, **36**, No. 3, 60–68 (1995).
7. A. S. Fonarev, "A profile in a transonic stream under the action of wind gusts and weak shock waves," *Prikl. Mekh. Tekh. Fiz.*, **34**, No. 3, 20–27 (1993).
8. M. A. Naida and A. S. Fonarev, "Wave drag of bodies of revolution in a nonsteady transonic stream," *Prikl. Mekh. Tekh. Fiz.*, **37**, No. 3, 35–44 (1996).
9. H. Ashley and M. Landahl, *Aerodynamics of Wings and Bodies*, Addison-Wesley Publ. Co., Reading, Mass. (1965).
10. B. E. Engquist and S. J. Osher, "Stable and entropy-satisfying approximations for transonic flow calculations," *Math. Comp.*, **34**, No. 19, 259–271 (1980).
11. N. N. Yanenko, *Method of Fractional Steps for Solving Multidimensional Problems of Mathematical Physics* [in Russian], Nauka, Novosibirsk (1967).
12. K. P. Petrov, *Aerodynamics of Aircraft Components* [in Russian], Mashinostroenie, Moscow (1985).